Hindawi
Advances in Civil Engineering
Volume 2023, Article ID 6270570, 14 pages
https://doi.org/10.1155/2023/6270570

Research Article

Study on Vertical Dowel Connections in Precast Walls

K. Karthikeyan[1], **M. Helen Santhi**[1] and **G. Senthil Kumaran**[2]

[1]*School of Civil Engineering, Vellore Institute of Technology, Chennai, Tamil Nadu, India*
[2]*Department of Civil Engineering & Construction, The Copperbelt University, Kitwe, Zambia*

Correspondence should be addressed to M. Helen Santhi; helensanthi.m@vit.ac.in and G. Senthil Kumaran; kumaran.gs@cbu.ac.zm

Received 23 November 2022; Revised 13 April 2023; Accepted 4 November 2023; Published 29 November 2023

Academic Editor: Alessandro Rasulo

Precast concrete wall connections using dowels are becoming more popular and effective these days due to their ease of installation and cost. In this study, one-third scale models of slender and intermediate precast walls with dowel connections and monolithic concrete walls were tested experimentally and numerically under lateral cyclic loads. The experiments on precast walls and monolithic walls were conducted on a loading frame of capacity 20 T and the cyclic loads were applied until the failure of the wall specimens. The numerical studies on walls were carried out using Abaqus.cae software, and the same cyclic loads were applied. The responses such as ultimate load, displacement, cracking pattern, ductility, and energy dissipation capacity of precast walls were compared. The results obtained from the numerical investigation proved to be effective in simulating the actual behavior of the studied precast and monolithic walls, thereby reducing the burden of doing physical tests on a huge number of precast wall specimens.

1. Introduction

Precast structures are becoming popular in developing countries like India to provide housing for all people in a quicker time. The precast technology is a workable solution for large-scale construction ensuring quality, safety, faster construction with less site disturbance, etc. Precast concrete systems can be either a skeleton frame or a wall frame structure. The wall frame structure has shear walls resist both the gravity and lateral loads, so the carpet area increases for the given plinth area. The shear walls are preferred where any type of lateral load is to be resisted.

Connections become the critical stress region in a precast system as it has to safely transfer the forces and moments from one member to the other without much damage. The connection design determines the feasibility of construction, strength, quality, and adaptability in the structure. The connections should ensure that the forces are transferred between the precast elements adequately. The connections can be of dry and wet type. In the case of dry connections, dowels are made to fit with the provisions in the adjoining member and grouting is used to fix them. In the case of wet connections, the joint is cast at the site. Mechanical joints are also preferred as they exhibit high strength, energy dissipation, and ductility characters.

The behavior of horizontal connections between wall panels using multiple shear keys was studied by Rizkalla et al. [1] and compared the responses with the monolithic wall. The connections with multiple shear keys showed 60% higher shear capacity than the monolithic wall. Soudki et al. [2, 3] conducted cyclic load test on six full-scale precast wall panels with mild steel connection and monotonic load test on one wall panel using five different horizontal connection details. The energy dissipation capacity of all the connections was found to be good and the ductility ratio was in the range of 4–6. Crushing and spalling of the grout were observed in the connections. The shear walls have the characteristics such as high initial stiffness and lateral load capacity; they can be applicable as horizontal load-resisting members in the precast construction.

Frosch obtained the efficient connection details for the wall panels based on the cyclic test conducted on 14 precast wall panels. A design method was also developed for the optimum connection [4]. Lightweight sandwich panels used

in construction as enclosure elements were subjected to monotonic and cyclic full-scale shear testing by De Matteis and Landolfo [5] on both single-connection specimens and pin-jointed steel frames supported by infill panels.

Ile and Reynouard [6] proposed a constitutive model employing the idea of a smeared crack approach with orthogonal fixed cracks and assumed a plane stress condition and compared it to the experimental work for predicting the cyclic response of reinforced concrete (RC) structures. Another study reported by Hidalgo et al. [7] also on cyclic loading on precast walls highlighting the shear strength.

Lightly RC shear walls were subjected to static cycle experiments by Greifenhagen and Lestuzzi [8] in a scale of 1 : 3 for various horizontal reinforcement, axial force ratios, and concrete compressive strengths. The findings demonstrated that the deformation capacity of the lightly reinforced shear walls is substantial and unaffected by the horizontal reinforcement ratio. To ascertain the stiffness and strength of the loop joints using different parameters, Ryu et al. [9] conducted static loading tests and fatigue loading testing. It was discovered that the overlapping portion inside the loop junction had mechanical properties that are comparable to or rather preferable to those of the RC beam section devoid of joints.

On a large-scale model of a concrete shear wall with a flanged cross-section and a low proportion of vertical reinforcement, Adebar et al. [10] conducted cyclic load tests along a constant axial compression. According to research on the impact of cracking on effective stiffness, the ultimate failure mode was the buckling of an unsupported vertical reinforcing bar, which caused concrete to spall and the bar to break after a few postbuckling cycles. The wall's largest worldwide drift was 2.4%.

Six walls made of RC underwent quasistatic cycle tests by Dazio et al. [11]. The experimental findings demonstrated the significance of both the ductility and reinforcement content. Under cyclic loading, Smith et al. [12] tested a hybrid precast wall panel with mild steel and PT steel reinforcement and discovered that failure occurred prematurely at the joint between the wall's base and the foundation beam because the concrete's strength was less than specified and the confinement hoops were not positioned properly at the wall's toes. Thirty-four thin structural RC walls were evaluated under quasicyclic loads for Beyer et al.'s [13] study on the ratio of shear-to-flexural deformations. For shear walls whose shear-transfer mechanism is not weakening, it was discovered.

Smith et al. [12] used unbounded prestressing for horizontal connections. Confinement steel was provided in the walls, cyclic loads were applied on the specimen. Wall behaved as designed except the early failure of concrete parts. A gap opening was created b/w walls and foundation and shear slip of the panels was low. Prestressing helped to refill the gap and avoided slip of panels. Using an abaqus-based nonlinear finite element analysis under monotonic loads, Jin et al. [14] compared the seismic performance of wall-to-wall horizontal connections in precast shear walls to the monolithic walls. The computational results lead to the conclusion that the current connection technique's seismic performance, including its deformability and energy-dissipation capacity, is comparable to that of its cast-in-place counterpart.

Under lateral cyclic loads, insulated sandwich wall panels were studied by Hamid and Fudzee [15] for their seismic performance. The only indication of wall surface cracks on the specimens was the buckling of the aluminum channel. Twelve RC walls for low-rise dwellings were evaluated seismically. Carrillo and Alcocer [16] compared the seismic performance of these walls. Wall geometry, concrete type, web steel ratio, web reinforcement type, and testing method were the variables examined. Results from dynamic and QS-cyclic tests were compared, and it was found that stiffness and strength properties were influenced by the rate of loading, the failure mode-related strength mechanisms.

The behavior of precast wall connectors subjected to in-plane lateral ground movement was assessed by Vaghei et al. [17]. Steel and concrete nonlinear stress–strain behavior was used to model the wall. The connections started to crack, and the reinforcing hooks started to warp. One hundred percent of the combined strength of the spliced bars must be developed by the splice sleeve. The internal threading of the sleeve with 1/800-deep threads is sufficient to stop the grout from slipping out of the sleeve [18].

The bottom face horizontal joints are crucial because shear force transfer causes the most tension to be generated there. For the same grout characteristic, different types of geometry for horizontal connections result in different types of shear resistance. Shear connectors were used in the precast specimens subjected to cyclic loads by Wu et al. [19]. The precast walls' crack-resistance capabilities, load capacity, and energy dissipation were measured. We noticed low ductility because of the shear connectors. Two thin RC walls with a single layer of vertical and horizontal reinforcement were subjected to unidirectional (in-plane) and bidirectional (in-plane and out-of-plane) quasistatic cyclic testing by Rosso et al. [20]. The experiments revealed out-of-plane displacements that could cause the wall to break prematurely in-plane.

Peng et al. [21] used mortar sleeves for horizontal and vertical connections. Quasistatic test was performed on the specimens. Tensile stress was effectively transferred by steel sleeve with in-filled mortar. Peak loading capacity of precast shear walls was less than the theoretical value. Lago et al. [22] established horizontal connections with dowels at the end of the walls. It was observed that the detailing played a significant role in the ductility of walls. The precast walls behaved similarly to monolithic walls. Xu et al. [23] made horizontal connections using dowels and sleeves. Effective axial forces and lateral deformations were achieved for specimens put through quasistatic cyclic tests. Precast walls exhibited behavior akin to that of monolithic walls.

Members are sleek and slender in precast constructions and subtle to lateral forces. Strength and stiffness discontinuities may arise due to dry connections which will attract large distortions and damage to the joint under lateral loading [24].

Baek et al. [25] investigated the impact of reinforcing bars with 420 and 550 MPa on the shear strength of the shear wall when subjected to cyclic loading. Slender shear walls with 550 MPa bars behaved in a manner that was comparable

to walls with 420 MPa in terms of failure mechanism, safety margin, and average fracture width. To describe the nonlinear regime of the load–displacement relationship, Sørensen et al. [26] developed a second-order plasticity model. They presented their study of the shear behavior of two-sided dowel joints, which includes the initiation of dowel action at small shear displacements and the development of full catenary action in the reinforcement at large displacements.

By applying full-scale in-plane quasistatic cyclic loads, Zhu and Guo [27] examined two types of emulative precast concrete walls with dry horizontal connection and semidry horizontal connection. The monolithic wall's peak strength average was lower than that of the dry and semidry horizontal connections. The initial stiffness of the monolithic wall specimen was about 4%–6% higher in this horizontal connection than that of the precast specimens. Similar energy dissipation performance was shown by all specimens.

The shear resistance of precast wall connecting systems was studied by Pramodh et al. [28]. The relationship between load and deformation, maximum load carrying capacity, ductility, and energy dissipation were investigated. Dal Lago et al. [29] established horizontal connections by dowels at the end of the walls. Detailing played a major role in ductility of walls. Wall behaved similarly to monolithic walls.

Seifi et al. [30] created horizontal connections with metal ducts and dowels. The precast wall connections for grouted metal ducts that failed were employed. Stronger recommendations for grouted connection detailing have been made. As the axial load and wall length grew, it was discovered that the precast specimens' behavior was less desirable. It was found that using transverse reinforcement helped the walls respond better. Only when connections between precast pieces are expertly conceived and methodically performed can the long-term and sustainable operation of a structure be ensured [31]. The use of RC panels with concealed hollow slits and vertical slits is advised for the purpose of retrofitting older concrete or steel frames [32].

The technical foundation for the design, use, and construction of the laminated RC shear wall structure was provided by the numerical results obtained from abaqus.cae [33]. The precast specimens in this experiment had a similar bearing capacity and much greater ductility and deformation capacity than the control group [34, 35].

The previous study published by the authors was done to identify a suitable connection for slender walls which behave similar to monolithic walls in performance [36]. For the current investigation, slender and intermediate walls with and without SFRC near joints were adopted to avoid toe crushing under lateral loads. Both experimental and numerical investigations were performed for the current study.

The lateral load resistance characteristics of precast slender and intermediate wall connections using dowel bars under incremental cyclic loading were assessed in the current investigation.

2. Experimental Study

The precast specimen was selected considering the easiness and viability to execute in the field. In this study, connections between the wall panels were made using dowels. The performance of horizontal connections was evaluated under fixed axial load and incremental reversible lateral loads. Reduced scale models were used for the study. One-third model of the real-time structures was adopted based on the testing facilities available without compromising the height-to-length ratios given in IS 13920:2016 [35–37].

Two sets of specimens were used for the study, i.e., slender wall ($hw/lw > 2$) and intermediate walls ($1 \geq hw/lw \leq 2$) as per IS 13920:2016. Each set had a monolithic wall and two precast walls. The first type of precast walls had dowels uniformly distributed to transfer loads and uniform concreting. The second type precast walls had the same dowel arrangement as of the first type, but here fiber reinforced concrete (FRC) was used near the joints to avoid crushing of concrete under lateral loads.

The first set of walls was 400 mm long, 1,000 mm high, and 80 mm thick with a founding beam of cross-section 130 mm wide by 200 mm deep. The reinforcement was Φ6 mm bars spaced at 120 mm c/c on both faces (double mesh). The beam was provided with 4–Φ10 mm bars along the length and stirrups of diameter Φ6 mm at 100 mm c/c. The connection between the founding beam and the adjoining wall specimen is modeled to transfer moments to the base [35–37].

The second set of walls was 600 mm long, 1,000 mm high, and 80 mm thick with a founding beam of cross-section 130 mm wide by 200 mm deep. The reinforcement was Φ6 mm bars spaced at 120 mm c/c on both faces (double mesh). The beam was provided with 4–Φ10 mm bars along the length and stirrups of diameter Φ6 mm at 100 mm c/c.

2.1. Monolithic Walls (MWS and MWI). The monolithic walls MWS (Monolithic Wall—slender) and MWI ((Monolithic Wall—intermediate) served as reference walls to compare the performance of precast walls. The beam and the entire wall were cast monolithically in a single pour. The schematic arrangement of steel for monolithic wall is shown in Figures 1 and 2.

2.2. Precast Concrete Walls 1 (PCWS1 and PCWI1). The PCWS1 had three dowels uniformly placed in the wall, whereas PCWI1 had four dowels. Twelve millimeters dowels were used with a sufficient anchorage length in both the bottom and top parts. The top part of the wall was aligned with the bottom part and the sleeves were grouted using Conbextra GP2 grout material of strength 65 N/mm^2. The schematic arrangement of precast wall 1 is displayed in Figures 3 and 4.

2.3. Precast Concrete Walls 2 (PCWS2 and PCWI2). The sizes of the PCWS2 and PCWI2 specimens were in size to PCWS1 and PCWI1, respectively. Around 150 mm near the joints region was concreted with FRC. The FRC was made with 1.0% 3D fiber by weight of the binder. The schematic arrangement of precast wall 2 is displayed in Figures 5 and 6.

2.4. Testing. The walls were tested under a constant axial load and incremental cyclic load. Prior to applying a lateral force, a 1 MT axial load was delivered using a plate and roller setup.

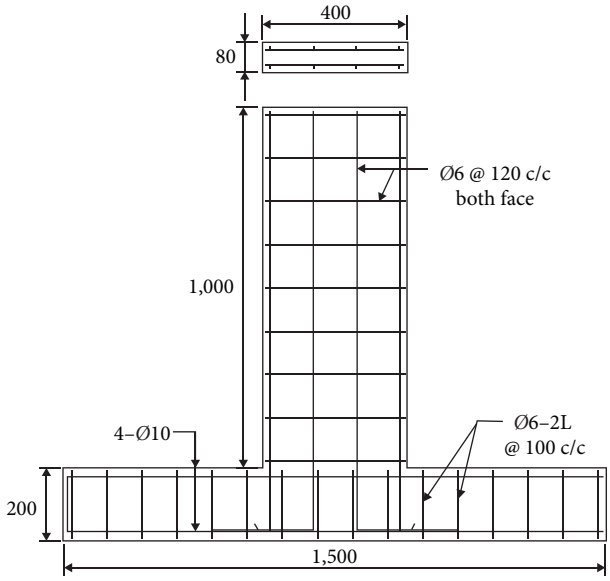

Figure 1: Monolithic wall panel—slender (MWS).

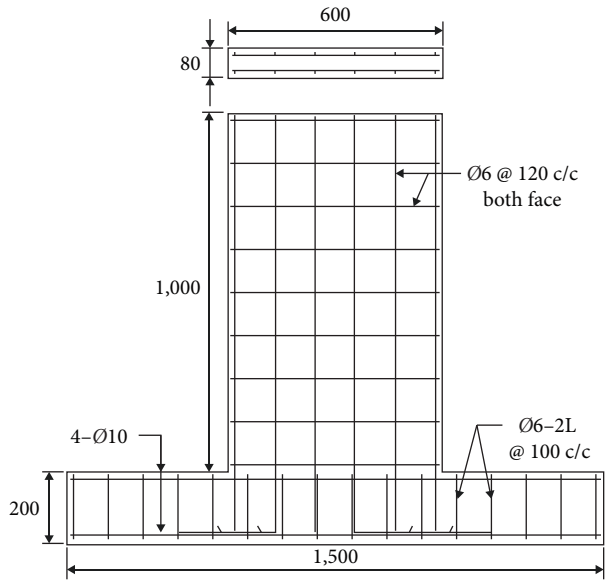

Figure 2: Monolithic wall panel—intermediate (MWI).

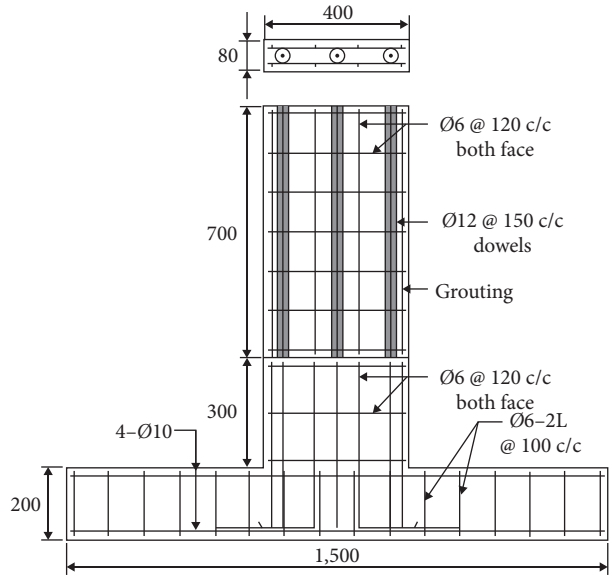

Figure 3: Precast wall panel—slender 1 (PWS1).

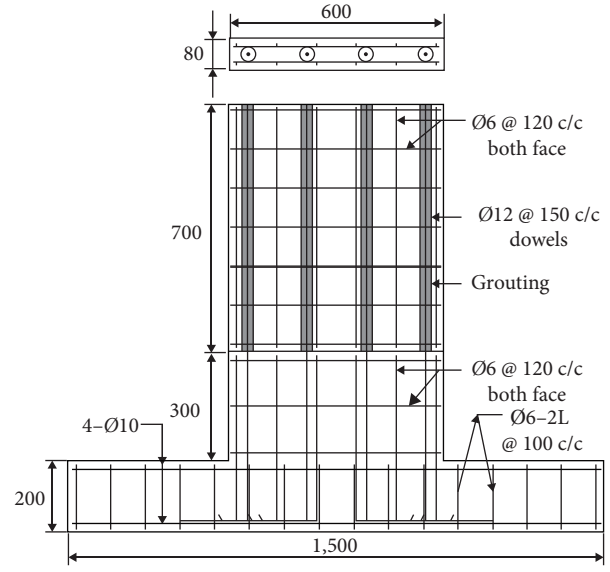

Figure 4: Precast wall panel—intermediate 1 (PWI1).

The lateral load in the form of displacement history was applied in increments using a displacement controlled 20 MT hydraulic jack. The displacement of 2 mm was maintained for each cycle till its failure. The corresponding loads were obtained for each cycle using a 20 MT load cell. Figure 7 shows the displacement history.

The deflections were measured using LVDTs placed at the loading points. Typical test setup is shown in Figures 8 and 9.

3. Numerical Investigation

The numerical models were developed for the monolithic walls and the precast walls in Abaqus-CAE 6.14 version using the same specifications as that of the experimental work and are shown in Figures 10–15. The concrete was modeled as solid element and reinforcing steel was modeled as wire. Meshing of size 20 mm was adopted.

3.1. Modeling. The concrete parts of the wall like the founding beam, wall were modeled drawn as lines and extruded to obtain the 3D model. The reinforcement parts like main bars, dowels, horizontal reinforcements, beam longitudinal bars, and stirrups were drawn as separate parts used as wire element. Material properties were assigned to concrete and steel, and the details are given in Table 1. The concrete elements were assigned with the properties of M30 concrete and FRC concrete. The steel wire elements were assigned with HYSD bar properties.

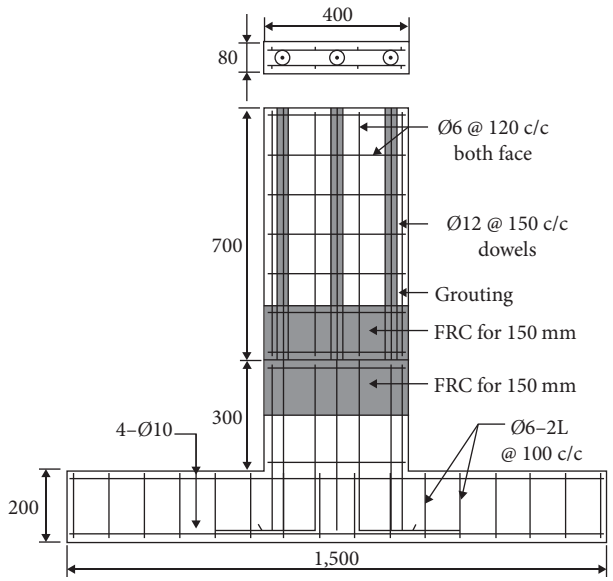

Figure 5: Precast wall panel—slender 2 (PWS2).

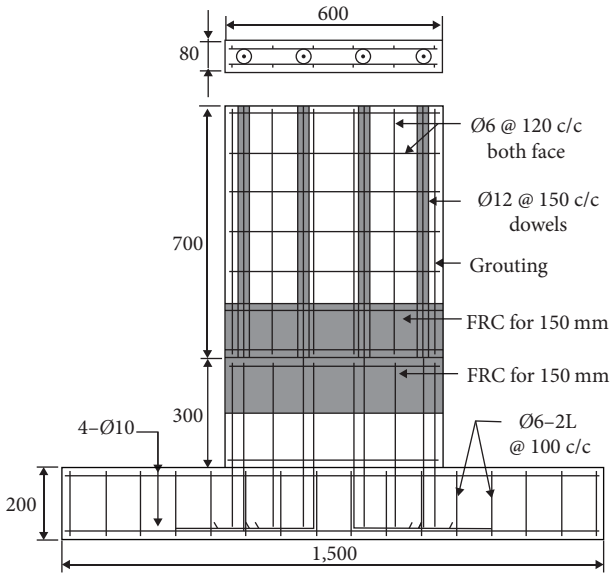

Figure 6: Precast wall panel—intermediate 2 (PWI2).

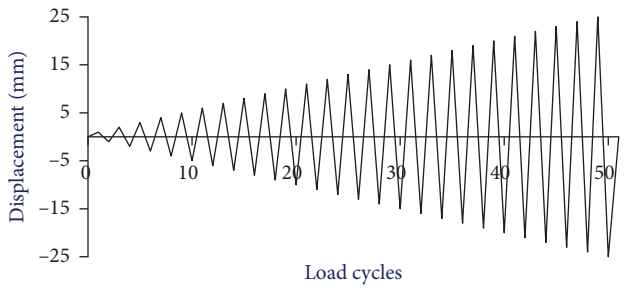

Figure 7: Displacement time history.

Figure 8: Test setup-typical.

Figure 9: Test setup-LVDT arrangement.

3.1.1. Assembly. The individual parts modeled were transferred to the assembly port one by one and were assembled as per their respective positions using transition, rotation, and array options. The array option was used for obtaining multiple elements such as stirrups. Embedment of reinforcement to the concrete was done using the embedment option considering concrete parts as the source of embedment.

3.1.2. Support and Loading. The base of the founding beam was provided with fixed support as in the experimental study. This support condition was achieved by arresting all the degrees of freedom at each point. The loading was given as displacement time history using amplitude command. The incremental cyclic loading was given as amplitude increasing and reversing for every second. The displacement history

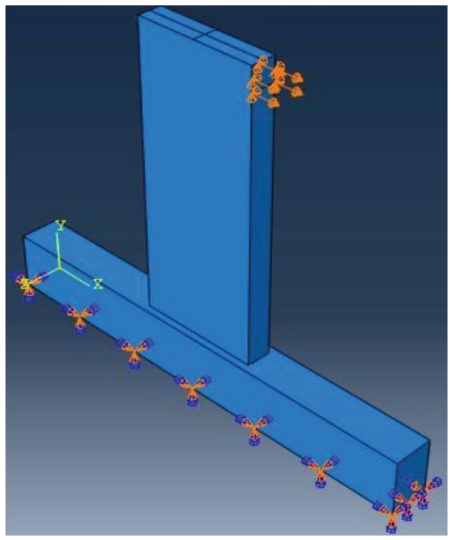

Figure 10: Monolithic wall panel—slender.

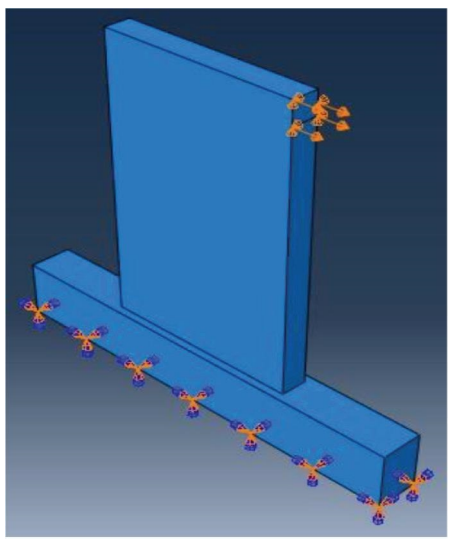

Figure 11: Monolithic wall panel—intermediate.

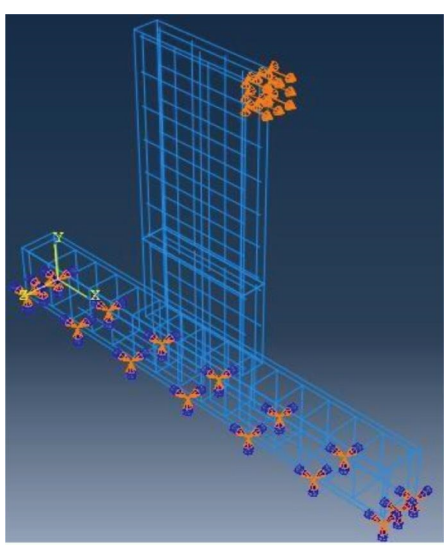

Figure 12: Precast wall panel—slender 1 (reinforcement detailing).

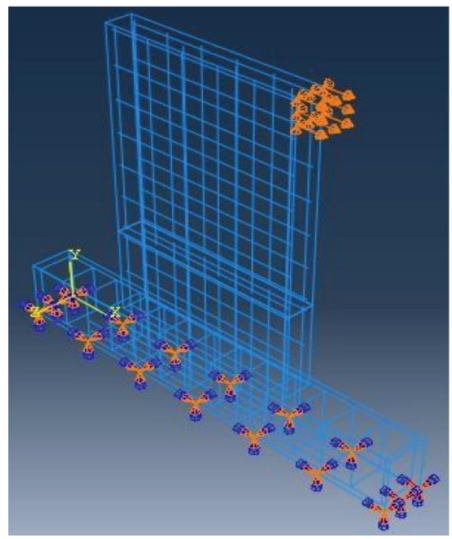

Figure 13: Precast wall panel—intermediate 1 (reinforcement detailing).

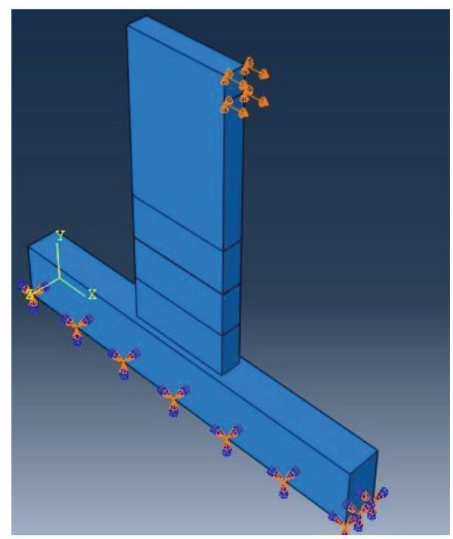

Figure 14: Precast wall panel—slender 1.

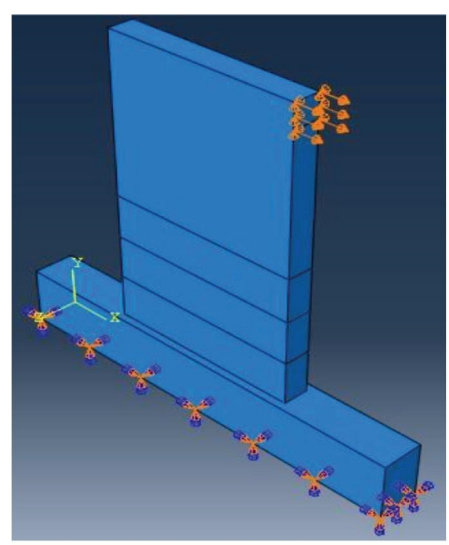

Figure 15: Precast wall panel—intermediate 1.

Table 1: Material property for analysis.

Property	Concrete	Rebar
Grade	M 30	Fe 500
Density	24 kN/m^3	78.5 kN/m^3
Young's modulus (E)	27,384 N/mm^2	2 x 10^5 N/mm^2
Poisson's ratio	0.2	0.3

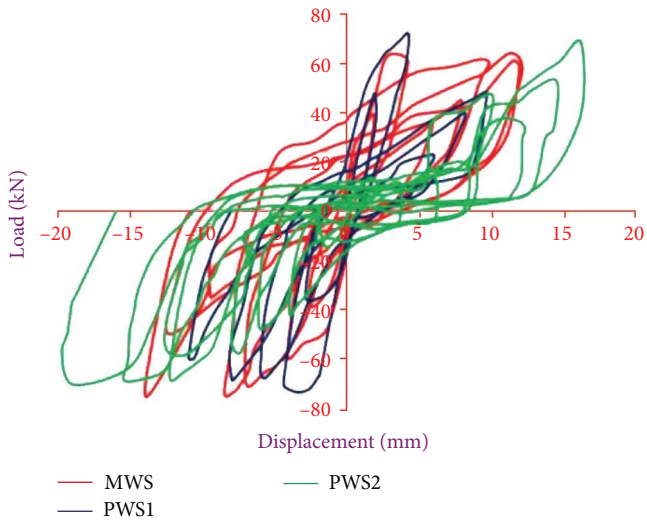

Figure 16: Load vs. displacement of slender wall panels (experiment).

was given at the top of the wall as provided in the experimental investigation.

3.1.3. Meshing. The concrete elements were meshed as 3D rectangular mesh and the steel elements were meshed as truss elements. The size of the mesh was taken as 20 mm. The total number of mesh cells for slender wall panels was 8,875 and for intermediate walls was 10,875.

3.2. Analysis. The given displacement history was provided for 50 cycles each for a time period of 1 s. The analysis was run till the model reached failure.

4. Results and Discussion

4.1. Experimental Investigation Results

4.1.1. Load versus Displacement Behavior. All the walls were loaded up to failure. The load versus displacement plots are shown in Figures 16 and 17 for all the specimens. The ultimate load and the corresponding deflection of the walls are shown in Tables 2 and 3. The ultimate loads of the precast walls PWS1 and PWS2 were 2.4% and 6.37% lesser than the slender monolithic wall (MWS), respectively. The ultimate loads of the precast walls PWI1 and PWI2 were 1.58% and 1.76% lesser than the intermediate monolithic wall (MWI), respectively. The precast walls were provided with dowels of bigger diameter compared to the wall mesh used in monolithic wall, which enables the precast walls to take loads like monolithic walls. In the case of monolithic wall, the steel reinforcement is distributed along its cross-section, whereas in the precast walls, the reinforcement at the joint is in the form of dowels and it is provided near the ends which helps in attaining the maximum load.

The deflections of all the precast walls were found to be much greater than the monolithic wall. This is because the precast walls were connected by dowels at the joint and they were able to slide over the bottom panel, which is one of the noted behaviors of precast wall panels. No out-of-plane bending or sliding of the wall panels was observed. The precast panels were still intact with the bottom panel even after the failure.

4.1.2. Failure Pattern. At the point where the foundation beam and wall meet, the monolithic wall had developed fissures. Due to reverse cyclic loads, the wall's two ends had fractured. The wall had no visible cracks. A cantilever action was displayed in the conduct. The wall panel joints in every precast wall had started to disintegrate. The wall panel junctions where the grouted panel joints were cracked. The precast wall specimens (PWS1 and PWI1) had witnessed the spalling of concrete at the junction due to crushing under compression from lateral loads whereas the precast wall specimens (PWS2 and PWI2) were witnessed only with cracks. The spalling of concrete did not occur in the PWS2 and PWI2 specimens as the junction was strengthened by using FRC on either side of the joint to avoid the crushing failure. The cracking pattern of walls is shown in Figures 18–23.

4.1.3. Ductility. The ductility factor of the specimens has been given in Tables 4 and 5. It was found that the precast specimens PWS1, PWS2, PWI1, and PWI2 had 9.57%, 42.86%, 27.78%, and 25.08% more ductile than the corresponding monolithic walls, respectively, which is a much needed behavior under seismic loading. The intermediate walls had similar ductility behavior irrespective of the material, whereas the slender walls behaved differently with and without FRC at joint regions.

4.1.4. Energy Dissipated. Energy dissipation can be measured as the area under the load–displacement curve. Tables 6 and 7 show the energy dissipation of the specimens. The precast specimens PWS1, PWS2, PWI1, and PWI2 had 17.56%, 2.74%, 1.72%, and 11.75% lesser energy dissipation than the corresponding monolithic walls, respectively, from the experimental investigation. It was observed that the precast walls with FRC were flexible than that of walls with normal concrete.

4.1.5. Initial Stiffness and Final Stiffness. The skeleton curves were plotted to estimate the initial and final stiffness of the specimens, as shown in Figures 24 and 25, respectively, and the values are shown in Tables 8 and 9. The monolithic slender wall was stiffer initially than the corresponding precast specimens. It was found that there was not much difference between the monolithic intermediate wall the corresponding precast walls in terms of initial stiffness. Both the slender walls and the intermediate walls exhibited good final stiffness compared to the initial stiffness.

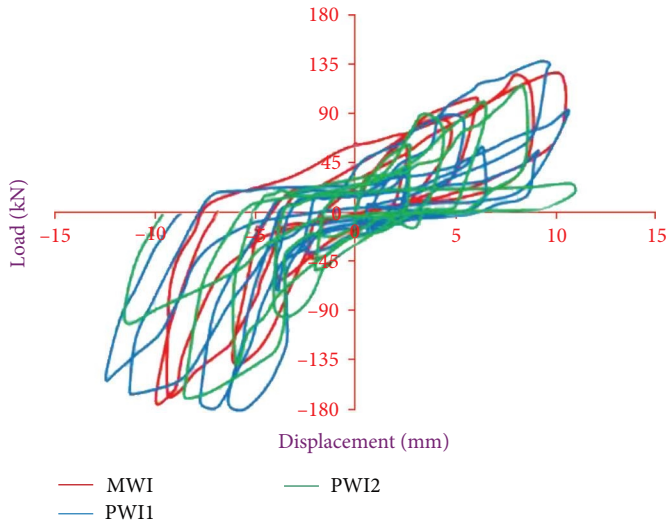

Figure 17: Load vs. displacement of intermediate wall panels (experiment).

Table 2: Ultimate loads of slender walls—experimental investigation.

Type	Ultimate load (kN)	Observation
MWS	75.30	—
PWS1	73.50	2.4% less than MWS
PWS2	70.50	6.37% less than MWS

Table 3: Ultimate loads of intermediate walls—experimental investigation.

Type	Ultimate load (kN)	Observation
MWI	170.90	—
PWI1	168.20	1.58% less than MWI
PWI2	167.90	1.76% less than MWI

Figure 19: Monolithic wall panel—intermediate—failure.

Figure 18: Monolithic wall panel—slender—failure.

Figure 20: Precast wall panel—slender 1—failure.

Figure 21: Precast wall panel—slender 2—failure.

Figure 22: Precast wall panel—intermediate 1—failure.

Figure 23: Precast wall panel—intermediate 2—failure.

Table 4: Ductility ratio of slender wall panels—experimental investigation.

Type	Ductility ratio	Observation
MWS	7.21	—
PWS1	7.90	9.57% more than MWS
PWS2	10.30	42.86% more than MWS

Table 5: Ductility ratio of intermediate wall panels—experimental investigation.

Type	Ductility ratio	Observation
MWI	7.38	—
PWI1	9.43	27.78% more than MWI
PWI2	9.23	25.08% more than MWI

Table 6: Energy dissipation of slender wall panels from experimental investigation.

Type	Energy dissipation (kN mm)	Observation
MWS	362.91	—
PWS1	309.23	17.56% less than MWS
PWS2	352.95	2.74% less than MWS

Table 7: Energy dissipation of intermediate wall panels from experimental investigation.

Type	Energy dissipation (kN mm)	Observation
MWI	794.48	—
PWI1	780.80	1.72% less than MWI
PWI2	701.14	11.75% less than MWI

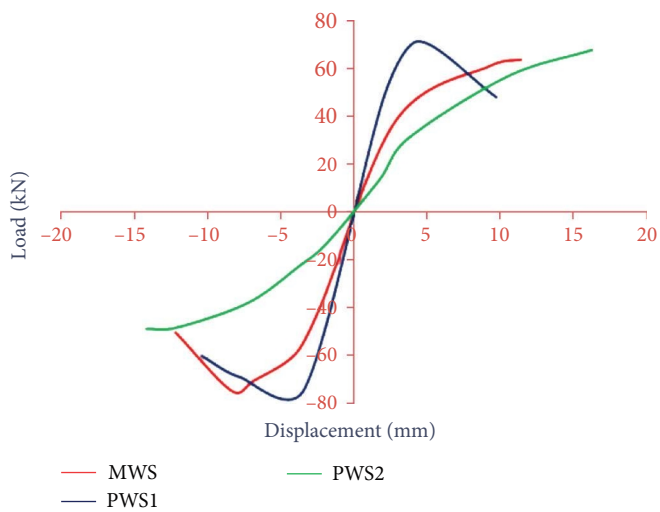

Figure 24: Slender wall panels—skeleton curve (experiment).

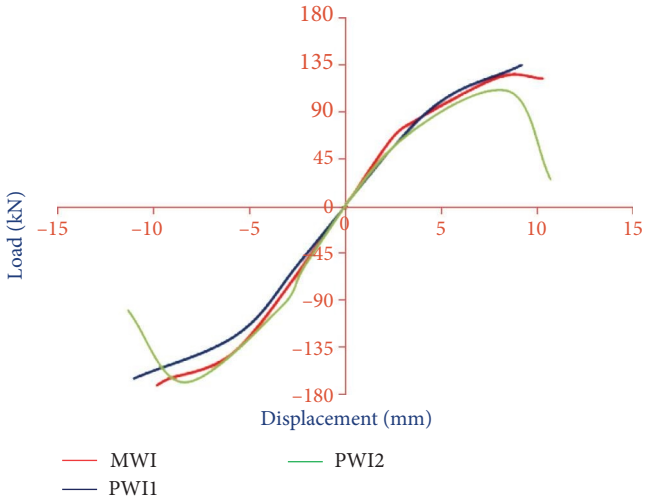

Figure 25: Intermediate wall panels—skeleton curve (experiment).

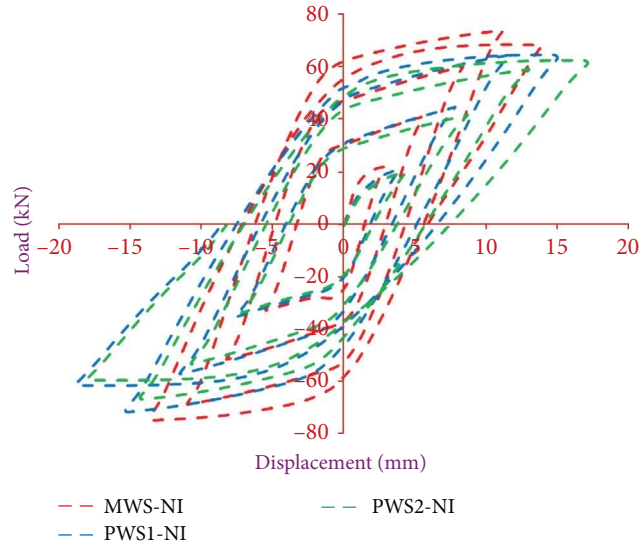

Figure 26: Load vs. displacement of slender wall panels (numerical).

Table 8: Stiffness degradation—slender wall panels.

Type	Elastic stiffness (kN/mm)	Secant stiffness (kN/mm)	Stiffness degradation (%)
MWS	17.98	8.76	51.27
PWS1	22.31	21.00	5.87
PWS2	7.22	4.15	42.52

Table 9: Stiffness degradation—intermediate wall panels.

Type	Elastic stiffness (kN/mm)	Secant stiffness (kN/mm)	Stiffness degradation (%)
MWI	26.41	17.26	34.64
PWI1	24.92	18.80	24.55
PWI2	24.09	19.99	17.01

4.2. Numerical Investigation Results

4.2.1. Load versus Displacement Behavior. All the walls were analyzed up to failure. The load versus displacement plots are shown in Figures 26 and 27 for all the specimens. The ultimate loads and the corresponding deflections of the walls are shown in Tables 10 and 11. The ultimate load of the slender precast walls PWS1 andPWS2 were 4.18% and 10.64% lesser than the monolithic wall—slender, respectively. The ultimate load of the intermediate precast walls PWI1 was 2.21% more and PWI2 was 3.24% lesser than the monolithic wall—intermediate, respectively.

4.2.2. Failure Pattern. The failure patterns obtained from the numerical investigation were comparable to the experimental investigation. The monolithic wall had failure at the junction of wall and base beam. The both ends of the wall had failed due to reverse cyclic loads. The precast wall specimens (PWS1 and PWI1) had witnessed the spalling of concrete at the junction due to crushing under compression from lateral loads, whereas the precast wall specimens (PWS2 and PWI2)

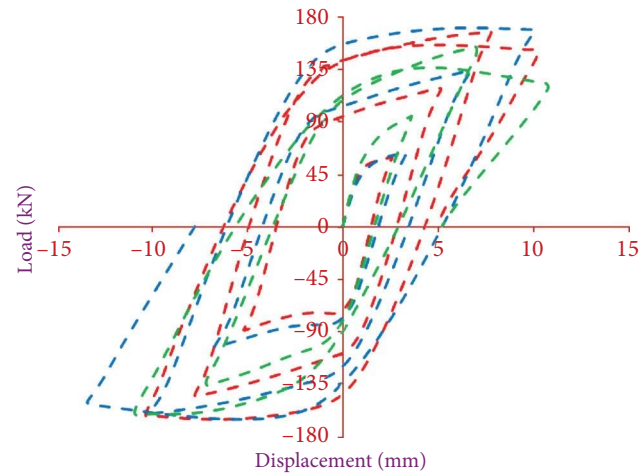

Figure 27: Load vs. displacement of intermediate wall panels (numerical).

Table 10: Ultimate loads of slender wall panels—numerical investigation.

Type	Ultimate load (kN)	Observation
MWS	74.35	—
PWS1	71.24	4.18% less than MWS
PWS2	66.44	10..64% less than MWS

Table 11: Ultimate loads of intermediate wall panels—numerical investigation.

Type	Ultimate load (kN)	Observation
MWI	165.78	—
PWI1	169.44	2.21% more than MWI
PWI2	160.41	3.24% less than MWI

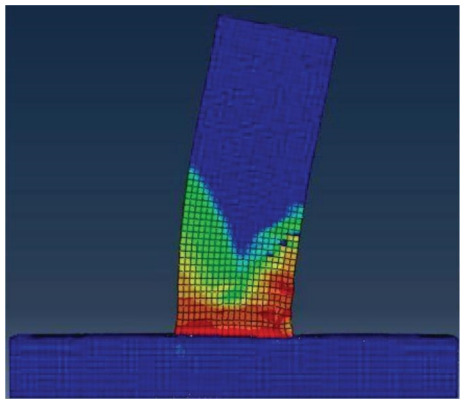

Figure 28: Failure patterns of MWS (numerical).

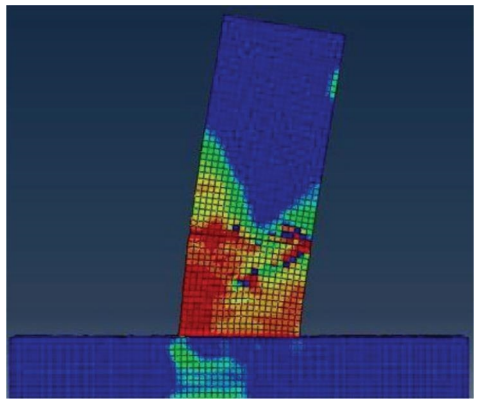

Figure 29: Failure patterns of PWS1 (numerical).

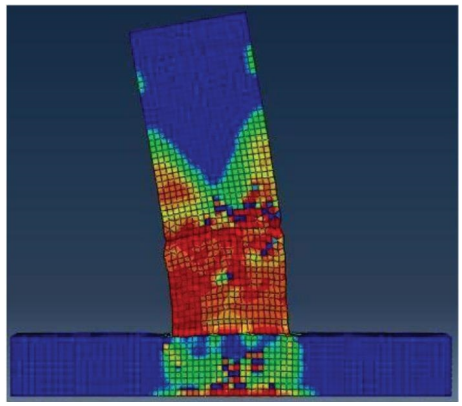

Figure 30: Failure patterns of PWS2 (numerical).

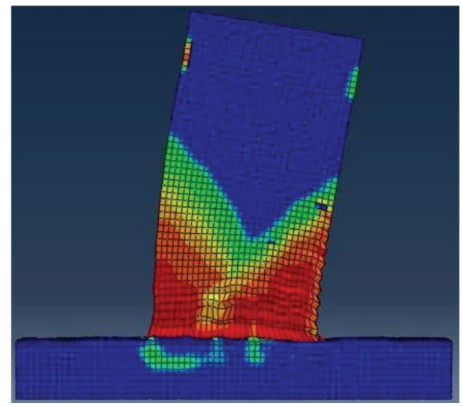

Figure 31: Failure patterns of MWI (numerical).

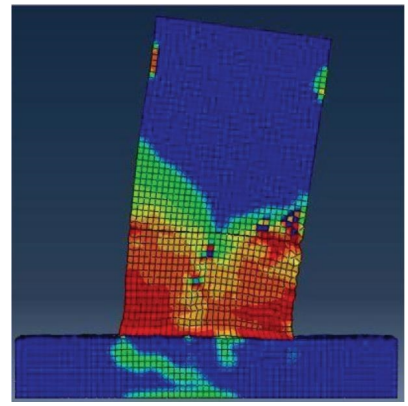

Figure 32: Failure patterns of PWI1 (numerical).

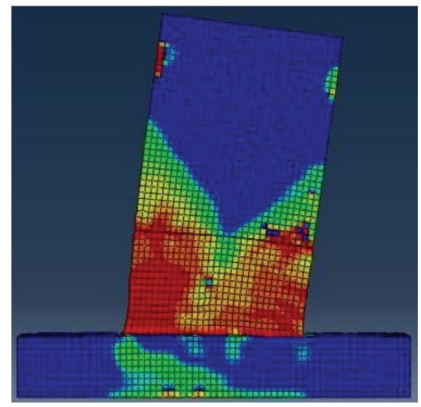

Figure 33: Failure patterns of PWI2 (numerical).

were witnessed only with cracks. The spalling of concrete did not occur in the PWS2 and PWI2 specimens as the junction was strengthened by using FRC on either side of the joint to avoid the crushing failure. The cracking pattern of walls is shown in Figures 28–33.

4.2.3. Ductility. The ductility factor of the specimens has been given in Tables 12 and 13. It was found that the precast specimens PWS1, PWS2, PWI1, and PWI2 had 13.23%, 23.95%, 11.53%, and 11.16% more ductile than the corresponding monolithic walls, respectively, through numerical investigation. The intermediate walls had similar ductility behavior irrespective of the material whereas the slender walls behaved differently with and without FRC at joint regions as in the case of experiments.

4.2.4. Energy Dissipation. Tables 14 and 15 show the energy dissipation of the specimens. The precast specimens PWS1,

Table 12: Ductility ratio of slender wall panels—numerical investigation.

Type	Ductility ratio	Observation
MWS	8.77	—
PWS1	9.93	13.23% more than MWS
PWS2	10.87	23.95% more than MWS

Table 13: Ductility ratio of intermediate wall panels—numerical investigation.

Type	Ductility ratio	Observation
MWI	9.42	—
PWI1	11.53	22.40% more than MWI
PWI2	11.16	18.47% more than MWI

Table 14: Energy dissipation of slender wall panels from numerical investigation.

Type	Energy dissipation (kN mm)	Observation
MWS	416.17	—
PWS1	343.15	14.78% less than MWS
PWS2	386.00	7.25% less than MWS

Table 15: Energy dissipation of intermediate wall panels from numerical investigation.

Type	Energy dissipation (kN mm)	Observation
MWI	808.60	—
PWI1	803.33	0.65% less than MWI
PWI2	800.30	1.03% less than MWI

PWS2, PWI1, and PWI2 had 14.78%, 7.25%, 0.65%, and 1.03% less energy dissipation than the corresponding monolithic walls, respectively, from the numerical investigation.

4.2.5. Initial Stiffness and Final Stiffness. The skeleton curves are shown in Figures 34 and 35, and the values are shown in Tables 16 and 17. The monolithic slender wall was stiffer initially than the corresponding precast specimens both in experimental and numerical investigations.

4.3. Influence of Fiber Reinforced Concrete (FRC). FRC concrete was used for a width of 150 mm on either side of PWS2 and PWI2 specimens. The test result of PWS2 was good in terms of protecting the edge region of the wall panels from excessive damage, crushing, vertical cracking, and spalling, which was observed in PWS1 as mentioned in the failure pattern. The FRC is beneficial in slender walls. The failure pattern of PWI1 and PWI2 was similar, i.e., only cracks were observed along the joint under lateral loading, which indicates that FRC is optional in intermediate walls.

4.4. Effect of Wall Length. When the length of the wall was increased from 400 to 600 mm, the lateral-load resistance and the energy-dissipation ability were increased more

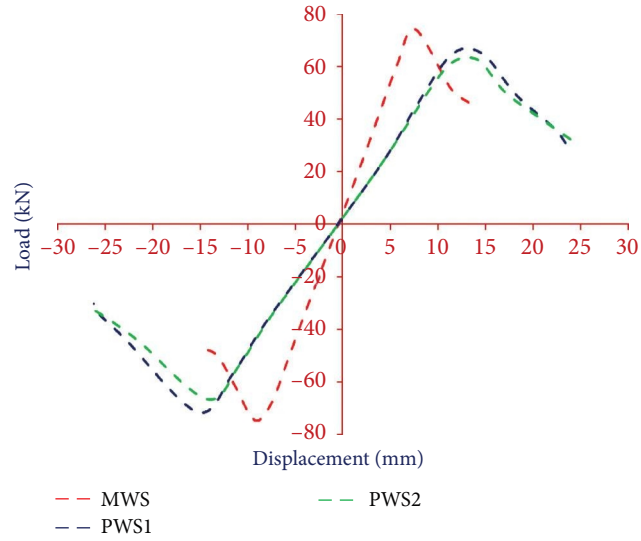

Figure 34: Slender wall panels—skeleton curve (numerical).

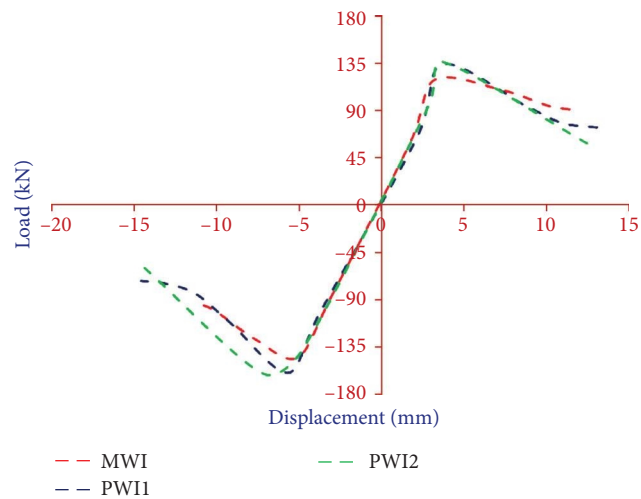

Figure 35: Intermediate wall panels—skeleton curve (numerical).

Table 16: Stiffness degradation of slender wall panels from numerical investigation.

Type	Elastic stiffness (kN/mm)	Secant stiffness (kN/mm)	Stiffness degradation (%)
MWS	9.58	8.04	16.07
PWS1	5.61	4.67	16.75
PWS2	4.97	4.65	6.43

Table 17: Stiffness degradation of intermediate wall panels from numerical investigation.

Type	Elastic stiffness (kN/mm)	Secant stiffness (kN/mm)	Stiffness degradation (%)
MWI	29.46	28.87	2.00
PWI1	29.78	28.51	4.26
PWI2	28.8	28.34	1.66

than two times. There was a difference in the failure pattern of the specimens also. The cracking, concrete crushing around the joint region, and spalling of concrete were detected in slender walls, whereas only cracking along the joints was observed in intermediate walls. This indicates that the slender walls will require more repair work compared to the intermediate walls when the concrete reaches its maximum ductile strength.

5. Conclusion

The following conclusions are made from the experimental and numerical investigations:

(1) The load carrying ability of the developed slender precast walls PSW1 and PWS2 was less than the slender monolithic wall MWS by 2.4% and 6.37%, respectively. Similarly, the intermediate precast walls PWI1 and PWI2 were also less than the intermediate monolithic wall MWI by 1.58% and 1.76%, respectively. This indicates that the load carrying capacities of the developed precast walls are close to the monolithic counterparts. Similarly, the load carrying capacity determined was also close to the experimental values.

(2) The ductility of the developed slender precast walls PSW1 and PWS2 was more than the slender monolithic wall MWS by 9.53% and 42.86%, respectively. Similarly, the intermediate precast walls PWI1 and PWI2 were also more than the intermediate monolithic wall MWI by 27.78% and 25.08%, respectively. It was found that the precast specimens PWS1, PWS2, PWI1, and PWI2 had 13.23%, 23.95%, 11.53%, and 11.16% more ductile than the corresponding monolithic walls, respectively. This indicates that the developed precast walls are also effective in resisting the lateral load as monolithic walls.

(3) The failure zones of the monolithic walls MWS and MWI were observed at the wallbeam junction, whereas failure zones for all the precast walls were at the junction of the wall panels as the junctions are the vulnerable locations of failure.

(4) The crushing of concrete was observed in the slender precast wall, PWS1, but only spalling of cover concrete was noticed in the PWS2. This is because of the joint regions were locally strengthened by FRC. The precast walls—intermediate without FRC had witnessed spalling of cover concrete, only cracks were observed for walls with FRC.

(5) The intermediate precast wall, PWI1, had spalling of cover concrete, whereas only mild cracking was observed in the intermediate precast wall, PWI2, which was locally strengthened by FRC at the joint regions. The use of FRC in intermediate walls has less impact than the slender walls.

(6) The precast specimens PWS1, PWS2, PWI1, and PWI2 had 17.56%, 2.74%, 1.72%, and 11.75% lesser energy dissipation than the corresponding monolithic walls, respectively, from the experimental investigation. The precast specimens PWS1, PWS2, PWI1, and PWI2 had 14.78%, 7.25%, 0.65%, and 1.03% less energy dissipation than the corresponding monolithic walls, respectively, from the numerical investigation. The results show that the precast walls with normal concrete were stiffer than the precast walls with FRC.

(7) The initial and final stiffness of all the walls were similar in both experimental and numerical investigations. The slender walls exhibited good final stiffness compared to the initial stiffness. Similarly, the final stiffness of the intermediate walls was also good compared to the initial stiffness.

(8) The numerical investigation can be adopted for determining the load carrying capacity, displacement, ductility, and stiffness degradation.

Data Availability

The data used to support the findings of this study are included within the article.

Conflicts of Interest

The authors declare that there are no conflicts of interest regarding the publication of this paper.

References

[1] S. H. Rizkalla, R. L. Serrette, J. S. Heuvel, and E. K. Attiogbe, "Multiple shear key connections for precast shear wall panels," *PCI Journal*, vol. 34, no. 2, pp. 104–120, 1989.

[2] K. A. Soudki, S. H. Rizkalla, and B. LeBlanc, "Horizontal connections for precast concrete shear walls subjected to cyclic deformations Part 1: mild steel connections," *PCI Journal*, vol. 40, no. 4, pp. 78–96, 1995.

[3] K. A. Soudki, J. S. West, S. H. Rizkalla, and B. Blackett, "Horizontal connections for precast concrete shear wall panels under cyclic shear loading," *PCI Journal*, vol. 41, no. 3, pp. 64–80, 1996.

[4] R. J. Frosch, "Panel connections for precast concrete infill walls," *ACI Structural Journal*, vol. 96, no. 4, pp. 467–472, 1999.

[5] G. De Matteis and R. Landolfo, "Structural behaviour of sandwich panel shear walls: an experimental analysis," *Materials and Structures*, vol. 32, no. 5, pp. 331–341, 1999.

[6] N. Ile and J. M. Reynouard, "Nonlinear analysis of reinforced concrete shear wall under earthquake loading," *Journal of Earthquake Engineering*, vol. 4, no. 2, pp. 183–213, 2000.

[7] P. A. Hidalgo, C. A. Ledezma, and R. M. Jordan, "Seismic behavior of squat reinforced concrete shear walls," *Earthquake Spectra*, vol. 18, no. 2, pp. 287–308, 2002.

[8] C. Greifenhagen and P. Lestuzzi, "Static cyclic tests on lightly reinforced concrete shear walls," *Engineering Structures*, vol. 27, no. 11, pp. 1703–1712, 2005.

[9] H.-K. Ryu, Y.-J. Kim, and S.-P. Chang, "Experimental study on static and fatigue strength of loop joints," *Engineering Structures*, vol. 29, no. 2, pp. 145–162, 2007.

[10] P. Adebar, A. M. M. Ibrahim, and M. Bryson, "Test of high-rise core wall: effective stiffness for seismic analysis," *ACI Structural Journal*, vol. 104, no. 5, pp. 549–559, 2007.

[11] A. Dazio, K. Beyer, and H. Bachmann, "Quasi-static cyclic tests and plastic hinge analysis of RC structural walls," *Engineering Structures*, vol. 31, no. 7, pp. 1556–1571, 2009.

[12] B. J. Smith, Y. C. Kurama, and M. J. McGinnis, "Design and measured behavior of a hybrid precast concrete wall specimen for seismic regions," *Journal of Structural Engineering*, vol. 137, no. 10, pp. 1052–1062, 2011.

[13] K. D. Beyer and M. J. N. Priestley, "Shear deformations of slender reinforced concrete walls under seismic loading," *ACI Structural Journal*, vol. 108, no. 2, pp. 167–177, 2011.

[14] Q. Jin, X. Dui, W. J. Zhao, T. G. Wu, and W. N. Guo, "Numerical analysis of seismic behavior of a new-type horizontal wall-to-wall connection for precast concrete shear walls," *Applied Mechanics and Materials*, vol. 353–356, pp. 3589–3592, 2013.

[15] N. H. A. Hamid and M. F. M. Fudzee, "Seismic performance of insulated sandwich wall panel under in-plane lateral cyclic loading," *Key Engineering Materials*, vol. 594-595, pp. 1020–1024, 2014.

[16] J. Carrillo and S. Alcocer, "Experimental investigation on dynamic and quasi-static behavior of low-rise reinforced concrete walls," *Earthquake Engineering & Structural Dynamics*, vol. 42, no. 5, pp. 635–652, 2013.

[17] R. Vaghei, F. Hejazi, H. Taheri, M. S. Jaafar, and A. A. A. Ali, "Evaluate performance of precast concrete wall to wall connection," *APCBEE Procedia*, vol. 9, pp. 285–290, 2014.

[18] E. Henin and G. Morcous, "Non-proprietary bar splice sleeve for precast concrete construction," *Engineering Structures*, vol. 83, pp. 154–162, 2015.

[19] D. Wu, S. Liang, M. Shen, Z. Guo, X. Zhu, and C. Sun, "Experimental estimation of seismic properties of new precast shear wall spatial structure model," *Engineering Structures*, vol. 183, pp. 319–339, 2019.

[20] A. Rosso, J. P. Almeida, and K. Beyer, "Stability of thin reinforced concrete walls under cyclic loads: state-of-the-art and new experimental findings," *Bulletin of Earthquake Engineering*, vol. 14, no. 2, pp. 455–484, 2016.

[21] Y.-Y. Peng, J.-R. Qian, and Y.-H. Wang, "Cyclic performance of precast concrete shear walls with a mortar-sleeve connection for longitudinal steel bars," *Materials and Structures*, vol. 49, pp. 2455–2469, 2016.

[22] B. D. Lago, M. Muhaxheri, and L. Ferrara, "Numerical and experimental analysis of an innovative lightweight precast concrete wall," *Engineering Structures*, vol. 137, pp. 204–222, 2017.

[23] G. Xu, Z. Wang, B. Wu et al., "Seismic performance of precast shear wall with sleeves connection based on experimental and numerical studies," *Engineering Structures*, vol. 150, pp. 346–358, 2017.

[24] H. Kothari, P. V. Patel, and D. Joshi, "Behaviour of the precast portal frames under lateral loading," *Asian Journal of Civil Engineering*, vol. 18, no. 7, pp. 1059–1076, 2017.

[25] J.-W. Baek, H.-G. Park, H.-M. Shin, and S.-J. Yim, "Cyclic loading test for reinforced concrete walls (aspect ratio 2.0) with grade 550 MPa (80 ksi) shear reinforcing bars," *ACI Structural Journal*, vol. 114, no. 3, pp. 673–686, 2017.

[26] J. H. Sørensen, L. C. Hoang, J. F. Olesen, and G. Fischer, "Testing and modeling dowel and catenary action in rebars crossing shear joints in RC," *Engineering Structures*, vol. 145, pp. 234–245, 2017.

[27] Z. Zhu and Z. Guo, "In-plane quasi-static cyclic tests on emulative precast concrete walls," *KSCE Journal of Civil Engineering*, vol. 22, pp. 2890–2898, 2018.

[28] R. Pramodh, V. Shripriyadharshini, and R. Vidjeapriya, "Shear behavior of horizontal joints between precast panels," *Asian Journal of Civil Engineering*, vol. 19, pp. 651–662, 2018.

[29] B. Dal Lago, P. Negro, and A. Dal Lago, "Seismic design and performance of dry-assembled precast structures with adaptable joints," *Soil Dynamics and Earthquake Engineering*, vol. 106, pp. 182–195, 2018.

[30] P. Seifi, R. S. Henry, and J. M. Ingham, "In-plane cyclic testing of precast concrete wall panels with grouted metal duct base connections," *Engineering Structures*, vol. 184, pp. 85–98, 2019.

[31] I. Holly and I. Abrahoim, "Connections and joints in precast concrete structures," *Slovak Journal of Civil Engineering*, vol. 28, no. 1, pp. 49–56, 2020.

[32] G. Sun, F. Li, and Q. Zhou, "Cyclic responses of two-side connected precast-reinforced concrete infill panels with different slit types," *Buildings*, vol. 12, no. 1, 2022.

[33] J. Li, Y. Wang, Z. Lu, and J. Li, "Experimental study and numerical simulation of a laminated reinforced concrete shear wall with a vertical seam," *Applied Sciences*, vol. 7, no. 6, Article ID 629, 2017.

[34] Z. Lu, Y. Wang, J. Li, and L. Wang, "Experimental study on seismic performance of L-shaped insulated concrete sandwich shear wall with a horizontal seam," *The Structural Design of Tall and Special Buildings*, vol. 28, no. 1, 2019.

[35] K. Karthikeyan, M. H. Santhi, and C. R. Chidambaram, "Behaviour of horizontal connections in precast walls under lateral loading," *International Journal of Recent Technology and Engineering*, vol. 8, no. 3, pp. 436–440, 2019.

[36] K. Karthikeyan and M. H. Santhi, "Experimental investigation on precast wall connections," *Journal of Advanced Research in Dynamical and Control Systems*, vol. 11, no. 6, pp. 1672–1678, 2019.

[37] S. Rohith, C. R. Chidambaram, K. Karthikeyan, and M. H. Santhi, "A study on hybrid precast walls," in *IOP Conference Series: Earth and Environmental Science*, vol. 80, pp. 1–6, 2017.